The Chemistry of Sulfoxy Species on Clean, Oxygenated, and Caesiated Ag{100}: A Study of Surface Reactivity by Fast XPS and TPR

ARTICLE *in* THE JOURNAL OF PHYSICAL CHEMISTRY B · SEPTEMBER 2001

Impact Factor: 3.3 · DOI: 10.1021/jp011883z

The Chemistry of Sulfoxy Species on Clean, Oxygenated, and Caesiated Ag{100}: A Study of Surface Reactivity by Fast XPS and TPR

Ashok K. Santra,[†] Daniel P. C. Bird,[†] E. Charles H. Sykes,[†] Federico J. Williams,[†] Andrea Goldoni,[‡] Alessandro Baraldi,[§] and Richard M. Lambert*,[†]

Department of Chemistry, University of Cambridge, Cambridge CB2 1EW, U.K., Sincrotrone Trieste, Basovizza, I-34012 Trieste, Italy, and Dipartimento di Fisica, Università di Trieste, I-34127, Trieste, Italy, and TASC−INFM Laboratory, I-34012 Trieste, Italy

Received: May 16, 2001

High-resolution XPS, including time- and temperature-dependent measurements, and temperature-programmed reactions, including ^{18}O isotope mixing studies, have been used to study the sulfoxy species formed on Ag{100} in the absence and presence of Cs. On the alkali-free preoxygenated surface, SO_2 adsorbs to form a surface sulfite which decomposes at ∼460 K releasing gaseous SO_2 and dissolved oxygen. Cs induces the formation of a more strongly bound alkali sulfite which reacts further to form alkali sulfate. The alkali sulfite and sulfate decompose at ∼525 and ∼575 K, respectively, releasing gaseous SO_2, dissolved oxygen, and a small amount of adsorbed sulfur. Isotope mixing data indicate that the sulfoxy species formed in the presence of alkali have a higher bond order with the Ag surface than the sulfite formed on the alkali-free surface. All these species are labile with respect to oxygen release in the temperature regime relevant to oxyanion-promoted ethene epoxidation, and a reaction scheme is proposed that accounts for their formation, interconversion, and decomposition.

Introduction

In many cases, the catalytic activity of transition metals is drastically altered by the presence of very low concentrations of gaseous SO_2 or of sulfur-containing compounds that act as SO_2 precursors. For example, sulfur-containing molecules in fuels result in SO_2 production which can poison automotive catalysts that contain platinum metals as the active component. Partly in recognition of such issues, a number of studies of SO_2 surface chemistry on single-crystal surfaces of various metals have been carried out, including Pt,[1,2] Cu,[3] Pd,[4] and Ni.[5] Although these effects of SO_2 are generally detrimental, this need not always be so. Thus, although SO_2 poisons Pt for the catalytic combustion of alkenes it actually promotes Pt in the combustion of alkanes. Studies on Pt{111} [6] have shown that this promotional effect is not just a consequence of an increase in support acidity due to SO_2 : important changes in the metal chemistry also occur. Adsorbed SO_4 is formed on the Pt surface and acts to activate dissociative alkane adsorption, the critical reaction initiating step for catalytic combustion.

Our interest in the surface chemistry of sulfoxy species on Ag stems from the apparently unique efficiency of silver in the catalytic epoxidation of terminal alkenes, especially ethene itself. Alkene epoxidation over pure silver-on-α-alumina catalysts is an important large scale industrial process.[7] Chlorine and alkali metals[8−11] enhance selectivity toward epoxide formation by modifying the surface chemistry of both the silver and the alumina components. Most recently, Bird et al.[12] demonstrated that a sulfoxy species produced by the adsorption of SO_2 on oxygenated Ag{100} both in the presence and in the absence of Cs-induced ultraselective epoxidation of styrene. Therefore, it is desirable to identify and characterize the various sulfoxy species formed on Ag in order to elucidate their role in alkene epoxidation catalysis.

Adsorption of SO_2 on clean and oxygen-covered Ag surfaces has been studied previously by XPS, TPR, HREELS, and NEXAFS.[13,14] It was shown that SO_2 adsorbs reversibly on clean Ag{110}, with a desorption rate maximum at ∼265 K;[13] in contrast, on the preoxygenated surface, adsorbed SO_3 and SO_4 were formed at higher temperature. In addition, Hofer et al. found that SO_2 interacted strongly with Cs/Ag{100}, desorbing at 650 K.[15,16]

Here we report high-resolution synchrotron fast XPS measurements (FXPS) on the evolution and thermal decomposition of the sulfoxy surface species generated by SO_2 chemisorption on clean and Cs-modified Ag{100} in the presence of oxygen. This technique was recently used to follow in real time the course of a relatively complex surface reaction: the trimerisation of acetylene to benzene on Pd{111}.[17] Only one core level (C 1s) was available; even so a rather detailed picture of the associated surface processes emerged. In the present case, the time and temperature evolution of three core levels (Cs 4d, O 1s, and S 2p) could be followed. This information, augmented by laboratory TPR data, provides a clear picture of the identity, thermal stability, and interrelationship between five chemically distinct S-containing adsorbed species that can be formed, depending on the conditions: S, SO_2, SO_3, $^{Cs}SO_3$, and $^{Cs}SO_4$.

Experimental Methods

Temperature-programmed reaction (TPR) experiments were performed in Cambridge in an ion-pumped UHV chamber operated at a base pressure of 2×10^{-10} Torr; this apparatus has been described in detail elsewhere.[18] Before each TPR

* Corresponding author. Tel: 44 1223 336467. Fax: 44 1223 336362. E-mail: RML1@cam.ac.uk.
[†] Department of Chemistry.
[‡] Sincrotrone Trieste.
[§] Dipartimento di Fisica and TASC−INFM Laboratory.

10.1021/jp011883z CCC: $20.00
Published on Web 09/19/2001

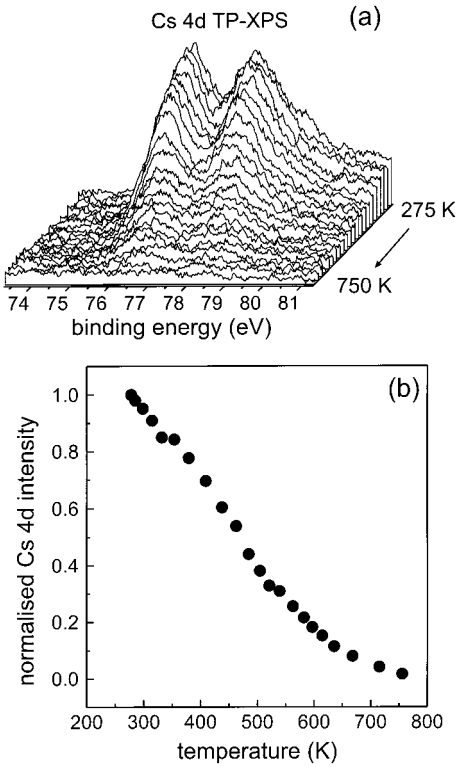

Figure 1. (a) Temperature-programmed Cs 4d spectra from a Cs-(0.2ML)/Ag{100} surface and (b) integrated Cs 4d intensity as a function of temperature.

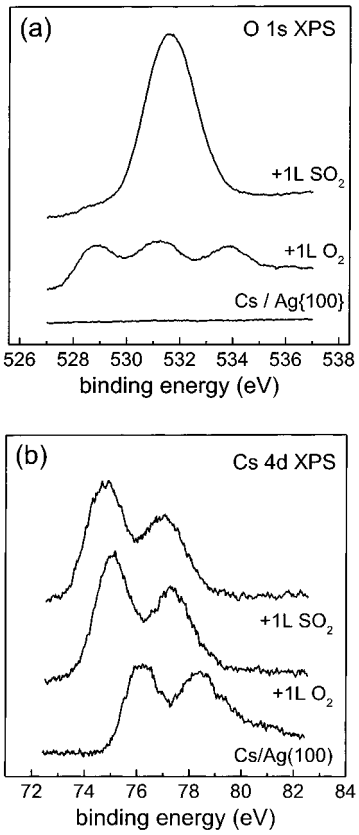

Figure 2. (a) O 1s and (b) Cs 4d spectra of clean Cs(0.2ML)/Ag-{100}, O_2(1L)/Cs(0.2ML)/Ag{100}. and SO_2(1L)/ O_2(1L)/Cs(0.2ML)/Ag{100} surfaces.

experiment, the Ag {100} crystal was Ar^+ sputtered, annealed to 800 K, and checked for surface cleanliness by Auger spectroscopy. Trace amounts of carbon were removed by repeated cycles of oxygen adsorption followed by heating to 800K while monitoring CO_2 desorption. The procedure was repeated until no CO_2 desorption was detectable. Oxygen and styrene were dosed via a calibrated tube doser and by backfilling the chamber, respectively.

Fast XPS studies were performed at the super-ESCA beamline[19−21] at the ELETTRA synchrotron radiation facility in Trieste, Italy. A double-pass hemispherical electron energy analyzer equipped with a 96 channel detector was used in the XP experiments, sample cleaning and gas dosing methods being identical to those employed in Cambridge. Surface order and cleanliness were checked by LEED and XPS, respectively. The angle between the analyzer entrance lens and the incident photon beam was 40° in the horizontal plane. Oxygen and Cs coverages were estimated by comparison of the corresponding XP spectra with those obtained for saturation coverages[22,23] of the two adsorbates. Temperature-programmed XPS experiments were performed by dosing reactants at 220 K and then ramping the temperature at approximately 0.3 K/s while monitoring the XP spectrum of the element of interest. The rate of FXPS data acquisition was ∼15 s/spectrum. TPR experiments were performed in a similar fashion, with a ramp rate of 8 K/s, while monitoring the relevant product masses by means of a quadrupole mass spectrometer whose ionizer was located ∼2 cm from the crystal face.

Results and Discussion

Cesium and Oxygen XP Spectra. Cs adsorption on Ag-{100} below 400 K results in a disordered overlayer.[15,16] Figure 1a shows high-resolution Cs 4d spectra from a 0.2 monolayer (ML) Cs-covered surface as a function of increasing temperature, after Cs deposition at 275 K. Figure 1b shows the temperature dependence of the integrated Cs 4d intensity derived from the data illustrated in Figure 1a. It is clear that Cs desorption from the clean surface is complete at > 750 K, in accord with published TPD data.[23] Such temperature-programmed FXPS data are complementary to TPR results and a combination of the two techniques can be very informative, as shown below.

Oxygen adsorption (1L) on the 0.2 ML Cs-covered Ag{100} surface at 220 K resulted in three distinct features in the O 1s spectrum, as shown in Figure 2a. Recall that, on clean Ag{100}, ∼2000 L of O_2 is required to saturate the surface. Preadsorbed Cs strongly catalyses the dissociative adsorption of oxygen, and although it reasonable to assume that with a 1 L O_2 dose most of the oxygen uptake occurs at Cs sites, we cannot exclude the possibility that some of the oxygen spills over onto the previously bare Ag surface. These are attributed to a suboxide of Cs, (528.5 eV) Cs_2O, (530.6 eV) and Cs_2O_2 (533.3 eV), respectively, in accord with the literature;[24,25] a contribution at ∼529 eV due to O_a could also be present, for the reason noted above. The corresponding Cs 4d peaks (Figure 2b) show a 1 eV shift to lower binding energy (BE) compared to the oxygen-free case, which is indicative of $Cs^0 \rightarrow Cs^+$ oxidation. SO_2 adsorption (1 L) on this oxygenated and caesiated surface at 220 K resulted in major changes in the O 1s emission which now consisted of a single broad peak at 531 eV; however, the Cs 4d spectrum showed little change. That is, once metallic Cs has been oxidized, the Cs 4d BE is insensitive to the identity of the chemical compound formed; this is in agreement with published BE values for wide range of Cs compounds (see, for example, refs 26 and 27). These results suggest that the three different Cs oxides reacted with SO_2 to yield sulfoxy species other than SO_2, a conclusion which receives strong confirmation

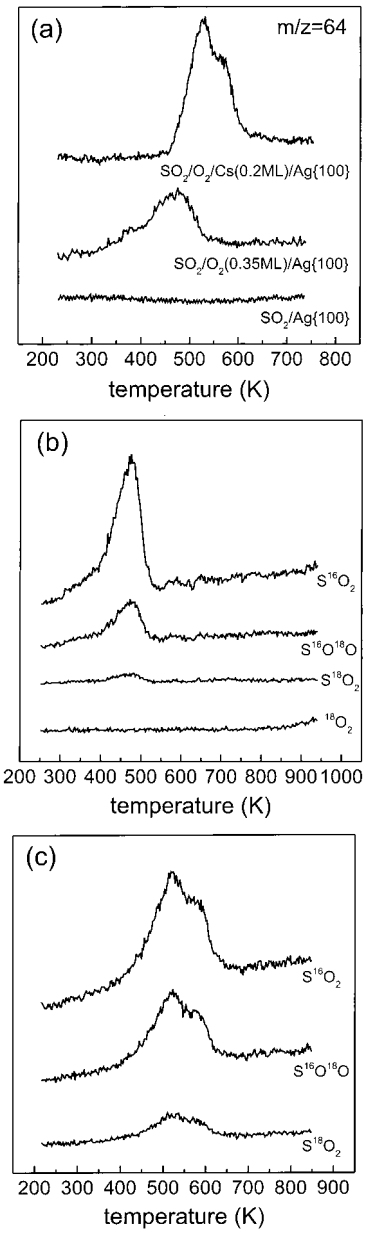

Figure 3. (a) TPR spectra for SO_2 ($m/z = 64$) from clean, O-precovered (0.35ML)/Ag{100}. and O_a/Cs(0.2ML)/Ag{100} surfaces. (b) $O_2$18 ($m/z = 34$) TPR spectra from $S^{16}O_2/^{18}O_a$/Ag{100} and (c) from $S^{16}O_2/^{18}O_a$/Cs(0.2ML)/Ag{100}.

from the S 2p XPS results described below which permit identification of the various species.

Temperature-Programmed Desorption and Reaction. TPD ($m/z = 64$; SO_2^+) for SO_2 desorption from clean Ag{100}, oxygenated Ag{100}, and Cs/Ag{100} are shown in Figure 3. In each case SO_2 adsorption was carried out at 250 K. Among other things, these results confirm that SO_2 does not adsorb on clean Ag{100} above 250 K, in agreement with the work of Outka et al. who reported desorption without decomposition below this temperature.[13] On the 0.35 ML oxygen-precovered surface an SO_2 desorption feature appeared at $T_p \sim 460$ K. However, SO_2 adsorption on the oxygen-saturated surface predosed with 0.2 ML of Cs resulted in *two* new desorption features at ~525 and ~575 K. The associated species may be identified by XPS and the relationships between them clarified by FXPS, as shown below.

The $m/z = 32$ TPR spectra always mirrored exactly the peak shapes and positions of the corresponding $m/z = 64$ (SO_2^+) spectra: accordingly, the $m/z = 32$ spectra are attributed to the mass spectral fragment ions SO_2^{2+} and S^+ from desorbing SO_2. Therefore, to determine unambiguously the fate of any residual O(a) formed in these experiments, they were repeated using $^{18}O_2$. Figure 3b shows the resulting $m/z = 36$ TPD spectra ($^{18}O_2^+$) which reveal that virtually no oxygen desorption occurred until >850 K, at which point the onset of desorption associated with dissolved oxygen [28] was just detectable; we shall return to this subject. Figure 3b also shows the TPR spectra for $m/z = 64$ ($S^{16}O_2$), 66 ($S^{16}O^{18}O$), and 68 ($S^{18}O_2$). Two observations can be made (i) the ratio of the $S^{16}O_2$:$S^{16}O^{18}O$ desorption yields is 4:1 and (ii) there is almost no $S^{18}O_2$ desorption. Above 250 K, the surface species responsible for the observed desorption peaks is SO_3 adsorbed on Ag, as clearly shown by the FXPS data presented below. Figure 3c illustrates the effect of Cs: TPR spectra for $m/z = 64$ ($S^{16}O_2$), 66 ($S^{16}O^{18}O$), and 68 ($S^{18}O_2$) from a $S^{16}O_2/^{18}O_2$/Cs/Ag{100} surface are shown. Here, the presence of Cs strongly affects the isotope distribution in the SO_2 product: (i) the $S^{16}O_2$:$S^{16}O^{18}O$ ratio is now 2:1 and (ii) a significant amount of $S^{18}O_2$ desorbs. These isotope mixing data provide additional clues about the nature of the sulfite species formed in the absence and presence of alkali. The lesser degree of isotope mixing observed in the absence of Cs suggests that the associated sulfite is mainly a monodentate species. (For example, in the limit of decomposition without isotope scrambling, one would expect $Ag-^{18}O-S^{16}O_2 \rightarrow Ag-^{18}O + S^{16}O_2$-(g)).

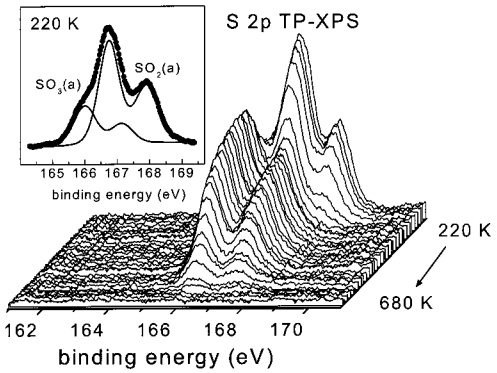

Figure 4. Temperature-programmed S 2p spectra from a SO_2(1L)/O_a-(0.35ML)Ag{100} surface. Inset show the curve-fitted S 2p spectrum at 220 K.

The two-peaked spectra observed in the presence of alkali suggest that alkali sulfite and alkali sulfate are indeed both formed, in excellent accord with the XPS results (see below). Moreover, the increased isotope mixing observed in this case suggests that tridentate sulfite and/or sulfate are present in substantial amounts.

S 2p and O 1s XPS: Identification of the Sulfoxy Species Formed on Ag{100} in the Absence of Coadsorbed Cesium. Figure 4 depicts the evolution of the high-resolution S 2p spectra obtained from a SO_2(1L)/O_2(0.35ML)/Ag{100} surface with increasing temperature (220−675 K). The inset shows a curve fitting of the first spectrum (220 K) in the temperature-programmed series. A very satisfactory fit is achieved with *two* S 2p doublets. The high energy component (S $2p_{3/2}$ 166.8 eV) is assigned to weakly bound molecular SO_2 at unmodified Ag sites: as noted above this species results from SO_2 adsorption on clean Ag at temperatures <250 K (this work and Outka et al.[13]). Although the O 1s and S 2p binding energies differ from those of the free molecule, as would be expected, the BE difference between the two levels is identical to that in gaseous SO_2.[13] The low BE component (S $2p_{3/2}$ 166 eV), which is present

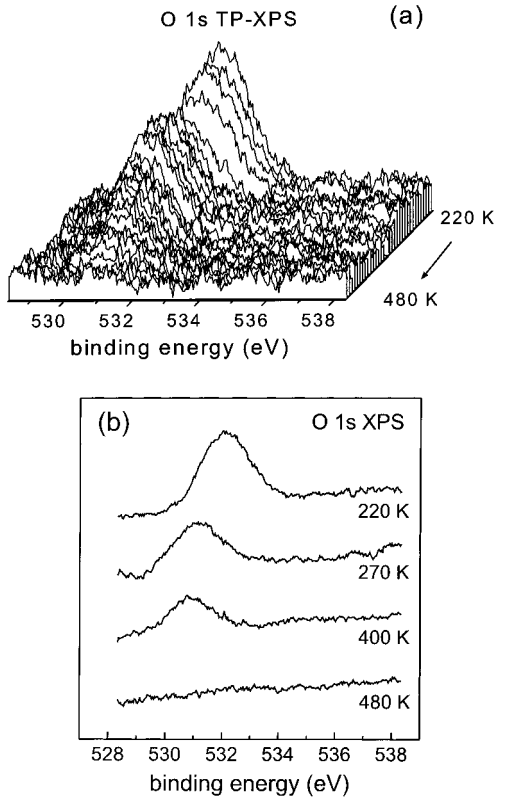

Figure 5. (a) Temperature-programmed O 1s spectra from SO_2(1L)/O_a(0.35ML)/Ag{100} and (b) O 1s spectra at four different temperatures from the same surface. Temperatures chosen to emphasize major spectral changes.

up to >350 K is assigned to a species resulting from interaction between SO_2 and O(a). Outka et al. observed a S $2p_{3/2}$ BE of 166.1 eV which they ascribed to SO_3 adsorbed on Ag{110}. We make the corresponding assignment: the S $2p_{3/2}$ BE (166 eV) emission is ascribed to SO_3, tentatively ascribed to a mainly monodentate species on the basis of the TPR isotope data described above. The associated reaction may be thought of in terms of a weakly adsorbed SO_2 hopping to an oxygen adatom site to yield SO_3(a) bonded to the surface via a single O atom, which would correspond to a monodentate surface silver sulfite. Note that the BE of SO_3 (S $2p_{3/2}$ 166.0 eV) does not correspond to that of the sulfite ion in bulk sulfites (Na_2SO_3, BE ~ 167.2 eV [29]). As we shall shortly see, a more stable adsorbed sulfite *is* formed under other conditions.

A complete set of the corresponding temperature-programmed O 1s FXPS data is shown in Figure 5a; Figure 5b shows just four of these O 1s spectra so as to provide a clearer indication of the changes occurring. Between 220 and 270 K the O 1s emission intensity decreased and shifted to lower BE. The decrease in intensity is due to desorption of weakly adsorbed molecular SO_2, as confirmed by the S 2p spectra shown in Figure 4. The shift toward lower BE is due to the conversion of SO_2 to SO_3 which takes place in the temperature interval 220−270 K as shown below. At 400 K the O 1s emission decreased in intensity due to SO_3 desorption. By 480 K the surface was oxygen-free, indicating complete SO_3 desorption and oxygen diffusion into the bulk, in agreement with the TPD data presented above.

The temperature dependence of the SO_2 and SO_3 integrated intensities derived from the data presented in Figure 4 is shown in Figure 6. It is apparent that molecularly adsorbed SO_2 undergoes reaction to produce SO_3 when the temperature is raised above 220 K, the process being completed by ~275 K.

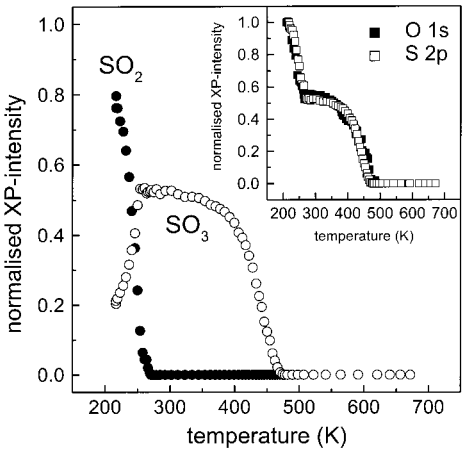

Figure 6. Relative intensity of SO_2(a) and SO_3(a) emission from SO_2-(1L)/O_a(0.35ML)/Ag{100} as a function of temperature. Inset shows temperature dependence of total integrated S 2p and O 1s intensities.

The SO_3 remained stable up to ~350 K at which point its coverage started to decrease, eventually reaching zero at 475 K. At this stage all S 2p photoemission was quenched. The inset to Figure 6 shows the temperature dependence of the *total* S 2p integrated intensity and that of the integrated O 1s intensity (derived from Figure 5a). These two quantities mimic each other very closely, the pronounced decrease between 220 and 275 K being due to desorption of molecular SO_2 from the surface. Both intensities decreased slowly between 275 and 350 K, at which temperature they decreased more rapidly, reaching zero at ~475 K. The final stage is attributed to decomposition of SO_3 as follows:

$$SO_3(a) \rightarrow SO_2(g) + O(\text{dissolved})$$

Given the well-known chemistry of the sulfur−oxygen system, we cannot rule out the possibility of equivalent though less likely decomposition pathways such as

$$2SO_3(a) \rightarrow S_2O_6(a) \rightarrow 2SO_2(g) + 2O(\text{dissolved})$$

Note that O(dissolved) rather than O(a) is proposed as the reaction product on the basis of the TPR data (Figure 3b) which show the onset of dissolved $^{18}O_2$ desorption at >850 K. In strong support of this view, the O 1s XP spectrum (Figure 5b) indicates the absence of surface oxygen at temperatures >475 K. The FXPS data accord well with the TPR results shown in Figure 3 in that the SO_2 desorption peak at ~460 K is undoubtedly associated with the decomposition of SO_3, as argued above. (The molecular SO_2 desorption observed at <250 K by FXPS does not appear in the TPR spectra because in this latter case gas dosing was carried out at 250 K). It is important to note that, in the absence of alkali, SO_4, readily identified by its S 2p BE of ~ 168 eV, was never observed. This stands in contrast to the results of Outka et al. [13] who found evidence for SO_4 formation on oxygenated Ag{110} in the absence of alkali.

S 2p and O 1s XP Results: Identification of the Sulfoxy Species Formed on Ag{100} in the Presence of Coadsorbed Cesium. SO_2 adsorption on the preoxygenated (1 L) and precaesiated (0.2 ML) Ag{100} surface resulted in complex S 2p spectra. The relevant temperature-programmed high-resolution S 2p spectra are shown in the main body of Figure 7. These spectra may be fitted using a minimum of five doublets. To aid visualization of the system's evolution, inset A shows curve-fitted spectra at three temperatures corresponding to very different populations of surface species. The spectrum obtained

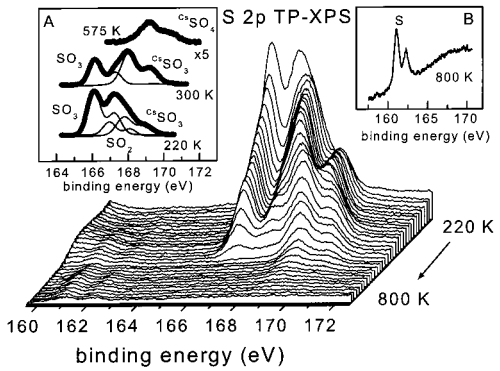

Figure 7. Temperature-programmed S 2p spectra from SO_2(1L)/O_a-(1L)/Cs(0.2ML)/Ag{100}. Inset A shows curve-fitted S 2p spectra at three different temperatures, chosen to emphasize major spectral changes. Inset B shows a six-scan average S 2p spectrum of the surface remaining after heating to 800 K.

immediately after SO_2 adsorption at 220 K can be fitted well with three doublets with S $2p_{3/2}$ binding energies of 166.0, 166.8, and 167.8 eV. The peaks at 166.0 and 166.8 eV are assigned to SO_3 and SO_2, respectively, in agreement with the results obtained in the absence of coadsorbed cesium. That at 167.9 eV is assigned to a new sulfite, identified as cesium sulfite on the basis of the S $2p_{3/2}$ BE of bulk Na_2SO_3 [S $2p_{3/2}$ 167.2 eV, ref 29]. For convenience, we designate this species as $^{Cs}SO_3$. Raising the temperature to 300 K results in (i) the expected disappearance of SO_2 (166.8 eV), (ii) a decrease in the SO_3 intensity (166.0 eV), and (iii) an increase in the intensity due to $^{Cs}SO_3$ (167.9 eV). Increasing the temperature to 575K resulted in formation of a surface species with S $2p_{3/2}$ BE of 169.2 eV. This can be assigned to Cs_2SO_4 [168.7 eV for Na_2SO_4, refs 30 and 31] and is therefore designated $^{Cs}SO_4$. The temperature dependence of the surface populations of these four species (Figure 9) is discussed below.

Inset B of Figure 7 shows the residual spectrum acquired after heating to 800 K. A new doublet with S $2p_{3/2}$ at 161.0 eV is formed that can be unequivocally assigned to S,[31] probably resulting from the reaction:

$$2^{cs}SO_4(a) \rightarrow S(a) + SO_2(g) + 6O(\text{dissolved})$$

(control experiments showed that S deposition was not the result of beam damage).

The corresponding temperature-programmed O 1s XP spectra obtained from the SO_2(1L)/O_2(1L)/Cs(0.2ML)/Ag{100} surface are shown in Figure 8a, a selected subset being shown in Figure 8b. It is clear that a progressive shift to higher BE occurred as temperature increases. This correlates with the progressive increase in oxidation state of S with increasing temperature (Figure 7). The O 1s spectrum observed at 570 K may be attributed to $^{Cs}SO_4$(a) alone, which had decomposed completely by 750 K, as established by the S 2p spectra (Figure 7, inset B). The analogous temperature-programmed Cs 4d spectra obtained from the SO_2(1L)/O_2(1L)/ Cs(0.2ML) /Ag{100} surface are illustrated in Figure 8c. Between 220 and 475 K the Cs 4d XP intensity remained constant. Increasing the temperature further caused a progressive decrease in the amount of Cs present: by ~775 K the surface was Cs-free.

The temperature dependence of the SO_2, SO_3, $^{Cs}SO_3$, and $^{Cs}SO_4$ integrated intensities derived from the data presented in Figure 7 is shown in Figure 9: the only species present at 220 K were SO_2, SO_3, and $^{Cs}SO_3$. Increasing the temperature from 220 to 275 K resulted in (i) a decrease in the coverage of both

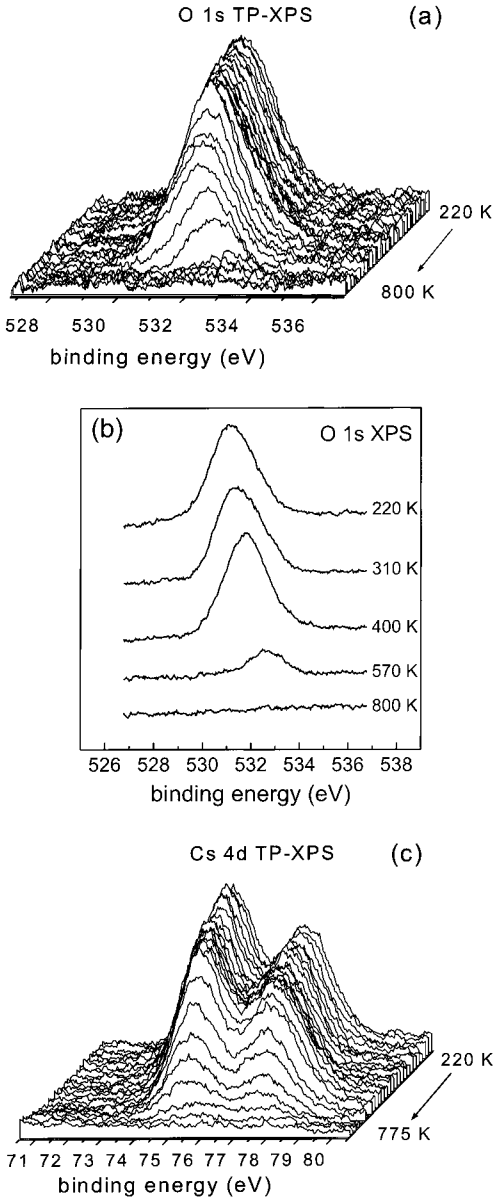

Figure 8. (a) Temperature-programmed O 1s spectra from SO_2(1L)/O_a(1L)/Cs(0.2ML)/Ag{100} and (b) O 1s spectra at four different temperatures from the same surface. Temperatures chosen to emphasize major spectral changes. (c) Temperature-programmed Cs 4d spectra from SO_2(1L)/O_a(1L)/Cs(0.2ML)/Ag{100}.

adsorbed SO_2 (which fell to zero at 275 K) and SO_3 and (ii) an increase in $^{Cs}SO_3$ coverage. These observations suggest that the following reaction occurred:

$$SO_3(a) \rightarrow {}^{Cs}SO_3(a)$$

Increasing the temperature to 350 K resulted in the appearance of sulfate, probably resulting from the reaction

$$^{Cs}SO_3(a) + O(a) \rightarrow {}^{Cs}SO_4(a)$$

Between 350 and 575 K the coverage of the two sulfite surface species decreased (reaching zero at 575 K), whereas that of the sulfate leveled off. Note that the decrease in sulfite coverage exceeds the increase in $^{Cs}SO_4$. This is due to partial decomposition of adsorbed sulfite to yield SO_2(g) (TPR peak at 525 K, Figure 3). Further increase in temperature from 575 to 800 K resulted in (i) a decrease in the cesium sulfate coverage

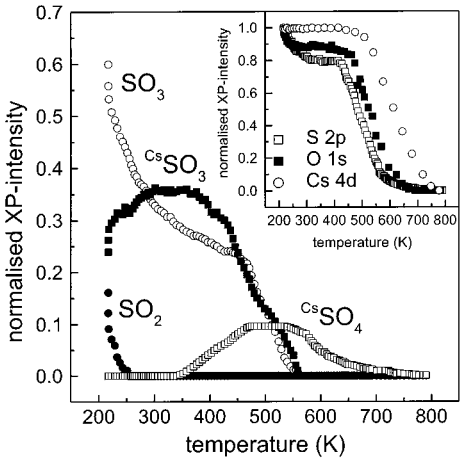

Figure 9. Normalized XP intensities of adsorbed SO_2 SO_3 $^{Cs}SO_3$ and $^{Cs}SO_4$ as a function of temperature. Inset shows changes in the total integrated S 2p, Cs 4d and O 1s intensities with respect to temperature for the same SO_2(1L)/O_a(1L)/Cs(0.2ML)/Ag{100} surface.

with release of SO_2(g) (TPR peak at 575 K, Figure 3) and (ii) the appearance of a small amount of sulfur (Figure 7, inset B**)**. These XPS results confirm that the two desorption peaks at 525 and 575 K (Figure 3a) are due to to $^{Cs}SO_3$ and $^{Cs}SO_4$ decomposition, respectively.

The inset to Figure 9 shows the overall behavior of the *total* integrated S 2p, O 1s, and Cs 4d intensities as a function of temperature (derived from Figures 7, 8a and 8c respectively). The S 2p and O 1s integrated intensities mimic each other very closely, the slight decrease between 220 and 275 K being due to desorption of molecular SO_2. Both intensities remained constant between 275 and 450 K, at which temperature they decreased more rapidly, reaching zero at ∼750 K. The final stage due is to decomposition of $^{Cs}SO_4$.

The initial slight decrease in the S 2p and O 1s signals between 220 and 275 K is not reflected in the Cs 4d intensity which remained constant up to ∼550 K: at this temperature the Cs 4d intensity decreased rapidly (mirroring the behavior of the S 2p and O 1s emission), reaching zero at ∼800 K.

S**ulfoxy Surface Chemistry of Silver in the Absence and Presence of Cesium.** The above scheme which summarizes the surface chemistry that results from SO_2 adsorption on clean, preoxygenated, and cesium+oxygen predosed Ag{100}is consistent with the TPR, XPS, and FXPS data. On the clean surface, SO_2 uptake below 250 K leads to weakly adsorbed molecular SO_2, which desorbs reversibly; no other species are formed. On oxygen precovered Ag{100}, SO_2 adsorption leads to simultaneous formation of both molecular SO_2(a) (166.8 eV) and a SO_3(a) (166.0 eV) the latter resulting from interaction of SO_2(a) with O(a). SO_3 is tentatively identified as a monodentate sulfite on the basis of the TPR results shown in Figure 3b. Increased temperature leads to partial desorption of SO_2(a), the rest of it undergoing further reaction with O(a) to form more SO_3(a). At temperatures above 350 K, the decomposition of SO_3 occurs to yield gaseous SO_2 and dissolved oxygen.

In the presence of preadsorbed oxygen *and* cesium, SO_2 adsorption at temperatures <250 K yields SO_2(a) (166.8 eV), SO_3(a) (166.0 eV), and $^{Cs}SO_3$(a) (167.9 eV). Raising the temperature results in one of two consequences for SO_2(a): either desorption below room temperature; or further reaction with O(a) yielding more SO_3(a) which itself subsequently converts to $^{Cs}SO_3$(a). This latter species reacts further with O(a) yielding $^{Cs}SO_4$(a) (169.2 eV). Finally, when the temperature exceeds 550 K, $^{Cs}SO_4$(a) decomposes to SO_2(g), leaving elemental S (161.0 eV) on the surface and dissolved oxygen, which latter is eventually released at high temperature (>850 K). We ascribe the 167.9 eV species to an alkali sulfite rather than the type of SO_4/Ag detected on alkali-free Ag{110}[13] (BE = 168 eV) for the following reasons. First, on Ag{100} the 167.9 eV species is only formed in the presence of alkali. Second, the observed BE is close to that of Na_2SO_3. Third, the 1.3 eV BE difference between this species and the 169.2 eV species assigned to Cs sulfate (which also appears only in the presence of Cs) is close to the BE difference of 1.5 eV reported for Na sulfite and sulfate.

It appears that the stability of sulfoxy anions on metal surfaces is quite strongly dependent on both the structure and chemical identity of the surface. On clean Pt{111},[32] SO_2 dissociates at low coverages, forming SO_2(a) only at high coverages. Preadsorbed oxygen immediately converts SO_2(a) to SO_4(a) without the intervention of the intermediate SO_3(a) stage. The SO_4(a) is stable to ∼550 K, eventually desorbing as SO_3(g), which relates interestingly to the well-known Pt-catalyzed industrial synthesis of SO_3 from SO_2 and O_2. Copper, less reactive than platinum but more reactive than silver, displays intermediate behavior. The sulfoxy surface chemistry of copper also exhibits an interesting resemblance to that of silver in terms of both structure sensitivity and in regard to the influence of elctropositive coadsorbates. Thus, with Cu{111}, Cu{100}, and Cu{110} Jackson et al. [33] Nakahashi et al. [34] and Pradier et al. [35] used, respectively, NIXSW, NEXAFS, and RAIRS to show that SO_2 immediately disproportionates on all three clean metal surface yielding a tridentate sulfite and elemental sulfur. In the case of Cu{110} [35] adsorption on the preoxygenated surface produced SO_4. Finally, the presence of a Mn overlayer on otherwise clean Cu{100}resulted in immediate SO_4 formation.[36]

Silver, least reactive of all, exhibits the greatest sensitivity to surface structure and to the effect of electropositive promoters. In the case of Ag{110}, the HREEL spectra obtained by Outka et al.[13] allowed them to identify both monodentate and bidentate SO_3 species, the former presumably closely related to the SO_3 species proposed here. The formation of bidentate SO_3 on the {110} surface versus the tridentate species proposed here (and detected on Cu{100}[34]) may principally reflect the difference in adsorption site symmetry on the 2-fold and 3-fold symmetric surfaces. Interestingly, on oxygenated Ag{110}, Outka et al.[13] found a monodentate to bidentate sulfite transition at ∼325 K, with the latter species stable to ∼500 K. This resembles the behavior reported here for the caesiated surface. Interestingly, in the absence of coadsorbed alkali, Outka et al.[13] also identified a stable sulfate which certainly does *not* form on Ag{100} under comparable conditions: in our case coadsorbed alkali is essential for sulfate formation. This is consistent with the relative base strengths (or work functions) of the {100} and {110} surfaces of Ag.

These findings are of significance with respect to oxy-anion promoted ethene epoxidation[11,37] where the following question arises. Does ultraselective epoxidation in the presence of coadsorbed oxo species such as those discussed here signify the opening of a new reaction channel involving direct oxygen transfer from the oxo species to the adsorbed alkene? Clearly, a labile SO_x(a)species which readily decompose to SO_{x-1}(a) + O may be catalytically significant in oxygen transfer reactions, and it is therefore interesting that all three sulfoxy species that we find on Ag{100} are labile with respect to oxygen release in the temperature regime relevant to oxyanion-promoted ethene epoxidation,. Moreover, the apparent differences in behavior between Ag{110} and Ag{100} surfaces suggests that in

practical applications of such chemistry the Ag particle size is likely to play a role in SO_x-promoted alkene epoxidation.

Conclusions

SO_2 adsorbs reversibly on clean Ag{100} while preadsorbed oxygen leads to the formation of a sulfite species, likely monodentate. No SO_4(a) is formed under these conditions, the sulfite decomposing at ~350 K to yield SO_2(g) and dissolved oxygen.

In the presence of both oxygen adatoms and preadsorbed Cs, SO_2 chemisorbs to form a more strongly bound sulfite whose S 2p core level binding energy corresponds to an alkali sulfite.

At ~350 K the surface Cs sulfite reacts further, unambiguously yielding a sulfate, which at ~550 K disproportionates to SO_2(g), sulfur, and dissolved oxygen.

^{18}O isotope mixing data indicate that the sulfoxy species formed in the presence of Cs have a higher bond order with the Ag surface than the sulfite formed on the alkali-free surface.

High-resolution fast XPS provides a valuable means of following the course of relatively complex surface reactions.

Acknowledgment. D.P.C.B. and E.C.H.S. acknowledge the award of EPSRC research studentships. F.J.W. acknowledges a research fellowship from the Cambridge University Oppenheimer Fund. A.K.S. acknowledges support from BP-AMOCO Chemicals plc. Financial support from the UK Engineering and Physical Sciences Research Council under Grant GR/M76706 is gratefully acknowledged.

References and Notes

(1) Sun, Y. M.; Sloan, D.; Alberas, D. J.; Kovar, M.; Sun, Z. J.; White, J. M. *Surf. Sci.* **1994**, *319*, 34−44.

(2) Polcik, M.; Wilde, L.; Haase, J.; Brena, B.; Comelli, G.; Paolucci, G. *Surf. Sci.* **1997**, *381*, L568-L572.

(3) Pradier, C. M.; Jacqueson, E.; Dubot, P. *J. Phys. Chem. B* **1999**, *103*, 5028−5034.

(4) Burke, M. L.; Madix, R. J. *Surf. Sci.* **1988**, *194*, 223−244.

(5) Brundle, C. R.; Carley, A. F. *Faraday Discuss. Chem. Soc.* **1975**, *60*, 51.

(6) Wilson, K.; Hardacre, C.; Lambert, R. M. *J. Phys. Chem.* **1995**, *99*, 13755−13758.

(7) Serafin, J. G.; Liu, A. C.; Seyedmonir, S. R. *J. Mol. Catal. A* **1998**, *131*, 157−168.

(8) Grant, R. B.; Lambert, R. M. *Langmuir* **1985**, *1*, 29−33.

(9) Grant, R. B.; Lambert, R. M. *J. Catal.* **1985**, *93*, 92−99.

(10) Tan, S. A.; Grant, R. B.; Lambert, R. M. *J. Catal.* **1987**, *106*, 54−64.

(11) Grant, R. B.; Harbach, C. A. J.; Lambert, R. M.; Tan, S. A. *J. Chem. Soc., Faraday Trans. 1* **1987**, *83*, 2035−2046.

(12) Bird, D. P. C.; Santra, A. K.; Lambert, R. M. *Catal. Lett.* **2001**. *In press.*

(13) Outka, D. A.; Madix, R. J.; Fisher, G. B.; Dimaggio, C. *J. Phys. Chem.***1986**, *90*, 4051−4057.

(14) Solomon, J. L.; Madix, R. J.; Wurth, W.; Stohr, J. *J. Phys. Chem.* **1991**, *95*, 3687−3691.

(15) Hofer, M.; Stolz, H.; Wassmuth, H. W. *Surf. Sci.* **1993**, *287*, 130−134.

(16) Hofer, M.; Stolz, H.; Wassmuth, H. W. *Surf. Sci.* **1992**, *272*, 342−346.

(17) Lee, A. F.; Wilson, K.; Middleton, R. L.; Baraldi, A.; Goldoni, A.; Paolucci, G.; Lambert, R. M. *J. Am. Chem. Soc.* **1999**, *121*, 7969−7970.

(18) Wilson, K.; Lee, A. F.; Hardacre, C.; Lambert, R. M. *J. Phys. Chem. B* **1998**, *102*, 1736−1744.

(19) Peterson, H. *Opt. Commun.* **1982**, *40*, 402.

(20) Jark, W. *Rev. Sci. Instrum.* **1992**, *63*, 1241−1246.

(21) Abrami, A.; Barnaba, M.; Battistello, L.; Bianco, A.; Brena, B.; Cautero, G.; Chen, Q. H.; Cocco, D.; Comelli, G.; Contrino, S.; Debona, F.; Difonzo, S.; Fava, C.; Finetti, P.; Furlan, P.; Galimberti, A.; Gambitta, A.; Giuressi, D.; Godnig, R.; Jark, W.; Lizzit, S.; Mazzolini, F.; Melpignano, P.; Olivi, L.; Paolucci, G.; Pugliese, R.; Qian, S. N.; Rosei, R.; Sandrin, G.; Savoia, A.; Sergo, R.; Sostero, G.; Tommasini, R.; Tudor, M.; Vivoda, D.; Wei, F. Q.; Zanini, F. *Rev. Sci. Instrum.* **1995**, *66*, 1618−1620.

(22) Fang, C. S. A. *Surf. Sci.* **1990**, *235*, L291-L294.

(23) Stolz, H.; Hofer, M.; Wassmuth, H. W. *Surf. Sci.* **1993**, *287*, 564−567.

(24) Carley, A. F.; Roberts, M. W.; Santra, A. K. *J. Phys. Chem. B* **1997**, *101*, 9978−9983.

(25) Podgornov, E. A.; Prosvirin, I. P.; Bukhtiyarov, V. I. *J. Mol. Catal. A* **2000**, *158*, 337−343.

(26) Allen, G. C.; Curtis, M. T.; Hooper, A. G.; Tucker, P. M. *J. Chem. Soc., Dalton Trans.* **1973**, 1677.

(27) Sharma, J.; Gora, T.; Rimstidt, J. D.; Staley, R. *Chem. Phys. Lett.* **1972**, *15*, 233.

(28) Boronin, A. I.; Koscheev, S. V.; Malakhov, V. F.; Zhidomirov, G. M. *Catal. Lett.* **1997**, *47*, 111−117.

(29) Turner, N. H.; Murday, J. S.; Ramaker, D. E. *Anal. Chem.* **1980**, *52*, 84.

(30) Lindberg, B. J.; Hamrin, K.; Johansson, G.; Gelius, U.; Fahlmann, A.; Nordling, C.; Siegbahn, K. *Physi. Scr.* **1970**, *1*, 286.

(31) Tibbetts, G. *J. Vac. Sci. Technol.* **1978**, *15*, 497.

(32) Wilson, K.; Hardacre, C.; Baddeley, C. J.; Ludecke, J.; Woodruff, D. P.; Lambert, R. M. *Surf. Sci.* **1997**, *372*, 279−288.

(33) Jackson, G. J.; Driver, S. M.; Woodruff, D. P.; Abrams, N.; Jones, R. G.; Butterfield, M. T.; Crapper, M. D.; Cowie, B. C. C.; Formoso, V. *Surf. Sci.* **2000**, *459*, 231−244.

(34) Nakahashi, T.; Terada, S.; Yokoyama, T.; Hamamatsu, H.; Kitajima, Y.; Sakano, M.; Matsui, F.; Ohta, T. *Surface Science* **1997**, *373*, 1−10.

(35) Pradier, C. M.; Dubot, P. *J. Phys. Chem. B* **1998**, *102*, 5135−5144.

(36) Lu, H.; Janin, E.; Davila, M. E.; Pradier, C. M.; Gothelid, M. *Surf. Sci.* **1998**, *408*, 326−334.

(37) Palermo, A.; Husain, A.; Lambert, R. M. *Catal. Lett.* **2000**, *69*, 175−179.